RESEARCH ARTICLE   **OPEN ACCESS**

Theoretical Relationships of Fluid and Flow Quantities in Composite Porous Layers

W.S. Almalki*, M.H. Hamdan**

*(Department of Mathematics, Umm al-Qura University, Saudi Arabia)
** (Department of Mathematical Sciences, University of New Brunswick, Saint John, Canada E2L 4L5)

ABSTRACT

In this work we consider the use of Brinkman's equation in describing viscous fluid flow through porous media, and its applicability in describing flow through layered porous media when permeability is low. While available formulations of viscous fluid flow over porous layers impose conditions of velocity and shear stress continuity at the interface between layers, the case of flow through layered media with low permeability requires a formulation that captures the low shear stress across layers. To this end, we consider a formulation of Brinkman's equation based on Williams' constitutive equations in order to take into account Brinkman's effective viscosity and how it influences the flow characteristics across the porous layers, and we derive theoretical relationships for fluid and flow quantities in composite porous layers.

Keywords – William's constitutive equations, porous layers, Brinkman equation

I. INTRODUCTION

Vafai and Thiagarajah [1] presented detailed analysis and classification of the following three fundamental problems and interface zones involving interface interactions in saturated porous media:

(I) Interface region between a porous medium and a fluid;

(II) Interface region between two different porous media;

(III) Interface region between a porous medium and an impermeable medium.

Interest in these three interface zones stems out of a large number of natural and industrial applications, including flow of groundwater in earth layers, flow of oil in reservoirs into production wells, blood flow through lungs and other human tissues, porous ball bearing, lubrication mechanisms with porous lining, in addition to heat and mass transfer processes across porous layers and their industrial applications (cf. [2], [3], [4], [5], and the references therein). More recently, there has been an increasing interest in turbulent flow over porous layers due to the importance of this type flow in environmental problems and water quality (cf. [6], [7], [8], and the references therein).

Vafai and Thiagarajah [1] contend that the problem of the interface region between a porous medium and a fluid has received the most attention. In fact, the last five decades have witnessed a large number of published articles dealing with this problem. This was initiated by the introduction of Beavers and Joseph [2] condition, which envisaged a slip-flow condition at a porous interface to replace the prior practice in porous bearing lubrication of using a no-slip condition at the interface. Their [2] use of Darcy's law as the governing equation of flow through the porous layer initiated a number of detailed investigations intended to:

- Analyze and derive the matching conditions to be used at the interface between the fluid layer and the porous layer, to better handle permeability discontinuity there.
- Validate and identify the most appropriate model that extends Darcy's law, yet provide compatibility of order with the Navier-Stokes equations that govern the flow in the fluid layer, and account for the presence of a thin boundary layer that inevitably develops in the porous layer (that is, in the sub-domain with the slower flow) when a viscous fluid flows over a porous layer.
- Account for the presence of a macroscopic, solid boundary that terminates a porous layer of finite depth, which gives rise to the need for porosity definition near the solid boundary in order to account for the channeling effect in the thin boundary layer near a solid wall.

The above and many other investigations point to a general agreement that conditions at the interface must emphasize (1) velocity continuity and, (2) shear stress continuity, in order to facilitate the matching of flow in the channel with the flow through the porous layer.

Many investigations point to the need for a non-Darcy model to govern flow through the porous layer. In particular, there has been an increasing interest in the use of Brinkman's equation, [9], as a viable and more appropriate model to govern the flow in the porous layer due to a number of short-comings of Darcy's law(cf. [3], [4], [5], [10], [11], [12], [13]). While Rudraiah [13] concluded that Brinkman's equation is a more appropriate model when the porous layer is of finite depth, Parvazinia *et al.* [12] concluded that when Brinkman's equation is used, three distinct flow regimes arise, depending on Darcy number (dimensionless permeability), namely: a free flow regime (for a Darcy number greater than unity); a Brinkman regime (for a Darcy number less than unity and greater than 10^{-6}); and a Darcy regime (for a Darcy number less than 10^{-6}). Their investigation [12] emphasized that *"the Brinkman regime is a transition zone between the free and the Darcy flows"*.

Related to flow through a channel underlain by a porous layer is the flow through layered media. This is the second interface zone identified and investigated by Vafai and Thiagarajah [1], and has been less studied. The use of a non-Darcy model in the study of flow through layered media was first considered by Vafai and Thiagarajah [1] who provided theoretical and experimental analysis to better understand the phenomenon and to validate some of the available results when a non-Darcy model is used. Vafai and Thiagarajah [1], Allan and Hamdan [14], and Ford and Hamdan [15], considered flow through two porous layers with the flow being governed by the same model or by two different models.

Many authors argue that Brinkman's equation is valid in the thin viscous region near a solid boundary or near the interface between flow regimes. In regions away from a solid boundary and away from a momentum transfer interface, Darcy's law is dominant and the regions fall into the Darcy regiments. This understanding is usually kept away from the problem formulation, and Darcy velocity is not taken into consideration. Instead, it has been customary to assume the same constant pressure gradient in each layer (or in the channel and the layer). In the current work we offer a modification to problem formulation by using the definition of the pressure gradient across each layer in terms of the Darcy velocity in the layer. This will shed further insights into the effects of permeability and Darcy velocity on the flow characteristics. Matching conditions on the velocity and shear stress at the interface between two layers are those developed by Williams [16] for flow over a porous layer.

This motivates the current work in which we consider flow through two porous layers that share an interfacial region, where the flow in each is governed by Brinkman's equation. We base our analysis on William's constitutive equations, [16], in order to provide a generalization and a formulation of the problem while taking into account Darcy's seepage flow rate. To this end, we consider the flow through a porous layer underlain by another porous layer and assume a sharp interface between the two layers. The lower layer is terminated from below, and the upper layer is terminated from above by solid walls (macroscopic boundary). The flow through each layer is assumed to be governed by Brinkman's equation with a different permeability for each layer, different flowing fluids, different layer thicknesses, and different viscosities. Conditions at the interface between layers are velocity continuity and shear stress continuity.

The objectives are to derive expressions for velocity and shear stress at the interface, to determine the velocity profiles in the layers; and to explore characteristics of the flow under these assumptions and for the above different characteristics. We derive relations characterizing the flow through two porous layers of differing permeabilities, differing thicknesses, differing fluids and flow conditions. An expression for the velocity at the interface is obtained and shows the dependence of this velocity on the Darcy numbers, porosities, base viscosities of the flowing fluids, the viscosity factors, and the thicknesses of the layers involved. A four-step procedure is outlined to obtain values for the parameters involved, and to completely determine the velocity at the interface.

II. PROBLEM FORMULATION

Consider the flow of two viscous fluids through two porous structures of different porosities and permeability. Each flow is assumed to be governed by the equation of continuity and Brinkman's equation, written here in a form based on the steady-state William's constitutive equations, [16], namely:

$$\nabla \bullet \varphi_i \vec{v}_i = 0 \qquad \qquad \dots(1)$$

$$\lambda_i \varphi_i{}^2 \mu_i \nabla^2 \vec{v}_i - \frac{\varphi_i{}^2 \mu_i}{k_i} \vec{v}_i - \varphi_i \nabla p_i = 0 \qquad \qquad \dots(2)$$

where $i = 1, 2$ refers to the *ith* porous medium, $\vec{v}_i$ is the velocity vector field, φ_i is the porosity, k_i is the permeability, μ_i is the fluid viscosity, and λ_i is a positive viscosity factor that is used to express the effective viscosity, μ_i^*, of the fluid in the porous medium to the base fluid viscosity, namely through a relation of the form:

$$\mu_i^* = \lambda_i \varphi_i^2 \mu_i. \qquad \qquad \text{... (3)}$$

For parallel flow through the composite porous layers in **Fig. 1**, equations (1) and (2) reduce to the following equations:

$$\frac{d^2 u_1}{dy^2} - \frac{u_1}{k_1 \lambda_1} = \frac{1}{\lambda_1 \mu_1 \varphi_1} \frac{dp_1}{dx} \; ; \; -L_1 \leq y < 0 \qquad \text{...(4)}$$

$$\frac{d^2 u_2}{dy^2} - \frac{u_2}{k_2 \lambda_2} = \frac{1}{\lambda_2 \mu_2 \varphi_2} \frac{dp_2}{dx} \; ; \; 0 < y \leq L_2. \qquad \text{... (5)}$$

Equations (4) and (5) are to be solved for $u_1(y)$ and $u_2(y)$, under the assumption of constant pressure gradients. The driving pressure gradients are typically taken as equal, however we will assume they are different, but there is pressure continuity at the interface. The pressure gradients are defined in terms of Darcy velocity by assuming Darcy's law to be valid in each layer. We will thus formulate the problem at hand using the Darcy velocity, Q_i. This is accomplished by casting Darcy's velocity in the *ith* layer in the form:

$$Q_i = -\frac{k_i}{\lambda_i \mu_i \varphi_i} \frac{dp_i}{dx} \qquad \text{...(6)}$$

which gives

$$\frac{dp_i}{dx} = -\frac{\lambda_i \mu_i \varphi_i}{k_i} Q_i. \qquad \text{...(7)}$$

y

Solid Wall; y=L2

Porous Layer 2

Porous Interface (y = 0)

Porous Layer 1

Solid Wall: y= - L1
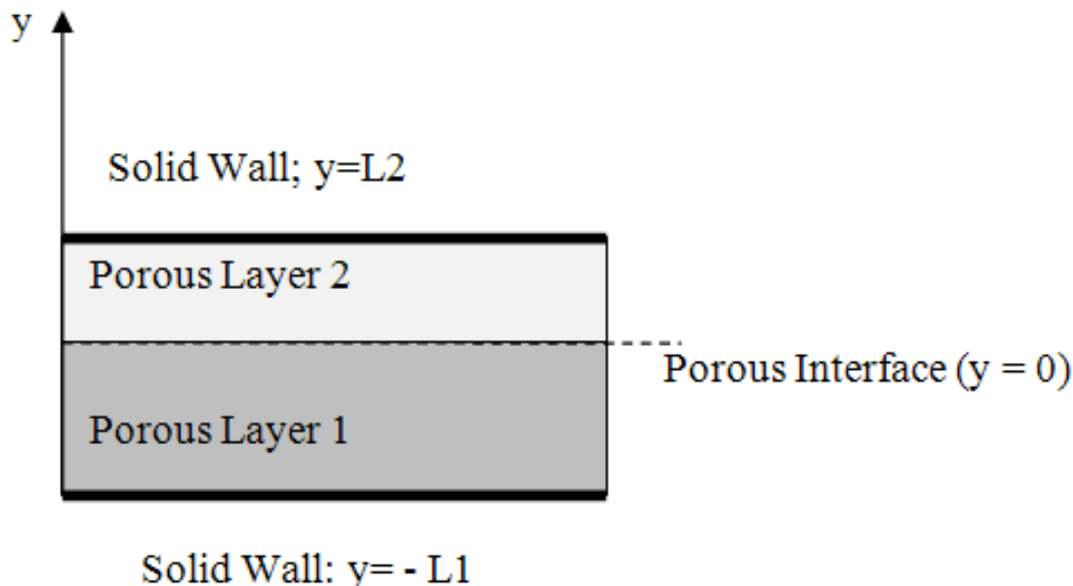
Figure 1. Representative Sketch of Flow through Two Porous Layers
Using (7) in (4) and (5) we obtain, respectively

$$\frac{d^2 u_1}{dy^2} - \frac{u_1}{k_1 \lambda_1} = -\frac{Q_1}{k_1} \; ; \; -L_1 \leq y < 0 \qquad \text{...(8)}$$

$$\frac{d^2 u_2}{dy^2} - \frac{u_2}{k_2 \lambda_2} = -\frac{Q_2}{k_2} \; ; \quad 0 < y \le L_2 . \tag{9}$$

Defining

$$\beta_i = -\frac{1}{k_i \lambda_i} \quad \text{and} \quad \alpha_i = -\frac{1}{k_i} \tag{10}$$

then equations (8) and (9) take the following forms, respectively:

$$\frac{d^2 u_1}{dy^2} + \beta_1 u_1 = \alpha_1 Q_1 \; ; \quad -L_1 \le y < 0 \tag{11}$$

$$\frac{d^2 u_2}{dy^2} + \beta_2 u_2 = \alpha_2 Q_2 \; ; \quad 0 < y \le L_2 . \tag{12}$$

Equations (11) and (12) are to be solved subject to the following conditions:

  a) No-slip velocity on macroscopic solid walls:

$$u_1(-L_1) = 0 \tag{13}$$

$$u_2(L_2) = 0 \tag{14}$$

  b) Velocity continuity at the interface between the two porous layers *(y = 0)*:

$$\varphi_1 u_1(0) = \varphi_2 u_2(0) . \tag{15}$$

  c) Shear stress continuity at the interface between the two porous layers *(y = 0):*
  In each layer, the fluid and the solid receive equal shear forces from the fluid in the other layer. The force exerted by each layer is given by:

$$\lambda_i \varphi_i^2 \mu_i \frac{du_i}{dy} , \; i=1, \, 2. \tag{16}$$

  At the interface *(y=0)* these forces are equal. Thus,

$$\lambda_1 \varphi_1^2 \mu_1 \frac{du_1}{dy} = \lambda_2 \varphi_2^2 \mu_2 \frac{du_2}{dy} . \tag{17}$$

III. SOLUTION TO THE GOVERNING EQUATIONS

General solution to equations (11) and (12) are given, respectively, by

$$u_1 = a_1 \cosh(\sqrt{-\beta_1} \, y) + b_1 \sinh(\sqrt{-\beta_1} \, y) + \frac{\alpha_1}{\beta_1} Q_1 \tag{18a}$$

$$u_2 = a_2 \cosh(\sqrt{-\beta_2} \, y) + b_2 \sinh(\sqrt{-\beta_2} \, y) + \frac{\alpha_2}{\beta_2} Q_2 \tag{18b}$$

where a_i, b_i, for *i*=1, 2, are arbitrary constants.
Using the no-slip conditions (13) and (14), we obtain, respectively:

$$a_1 \cosh(\sqrt{-\beta_1} L_1) - b_1 \sinh(\sqrt{-\beta_1} L_1) + \frac{\alpha_1}{\beta_1} Q_1 = 0 \tag{19a}$$

$$a_2 \cosh(\sqrt{-\beta_2} L_2) + b_2 \sinh(\sqrt{-\beta_2} L_2) + \frac{\alpha_2}{\beta_2} Q_2 = 0. \tag{19b}$$

Defining $Da_i = \dfrac{k_i}{L_i^2}$, the Darcy number in the *ith* layer, and using $\lambda_i = \dfrac{\alpha_i}{\beta_i}$, $\beta_i = -\dfrac{1}{k_i \lambda_i}$, we set

W.S. Almalki Int. Journal of Engineering Research and Applications
www.ijera.com
ISSN: 2248-9622, Vol. 6, Issue 2, (Part - 5) February 2016, pp.10-21

$$A_1 = \sqrt{-\beta_1}\, L_1 = \sqrt{\frac{L_1^{\,2}}{k_1 \lambda_1}} = \sqrt{\frac{1}{Da_1 \lambda_1}} \qquad \ldots(20a)$$

and

$$A_2 = \sqrt{-\beta_2}\, L_2 = \sqrt{\frac{L_2^{\,2}}{k_2 \lambda_2}} = \sqrt{\frac{1}{Da_2 \lambda_2}} \,. \qquad \ldots(20b)$$

Equations (19a) and (19b) can thus be written, respectively, as:

$$a_1 \cosh(A_1) - b_1 \sinh(A_1) + \lambda_1 Q_1 = 0 \qquad \ldots(21a)$$

$$a_2 \cosh(A_2) - b_2 \sinh(A_2) + \lambda_2 Q_2 = 0 \,. \qquad \ldots(21b)$$

Upon using condition (15) in (18a) and (18b) at *y = 0*, we obtain:

$$\varphi_1 (a_1 + \lambda_1 Q_1) = \varphi_2 (a_2 + \lambda_2 Q_2) \,. \qquad \ldots(22)$$

Solving (22) for a_2, we get

$$a_2 = \frac{\varphi_1}{\varphi_2}(a_1 + \lambda_1 Q_1) - \lambda_2 Q_2. \qquad \ldots(23)$$

Now, differentiating (18a) and (18b) with respect to *y* we obtain the following expressions for shear stress in layers *1* and *2*, respectively:

$$\frac{du_1}{dy} = a_1 \sqrt{-\beta_1}\, \sinh(\sqrt{-\beta_1}\, y) + b_1 \sqrt{-\beta_1}\, \cosh(\sqrt{-\beta_1}\, y) \qquad \ldots(24a)$$

$$\frac{du_2}{dy} = a_2 \sqrt{-\beta_1}\, \sinh(\sqrt{-\beta_2}\, y) + b_2 \sqrt{-\beta_1}\, \cosh(\sqrt{-\beta_2}\, y) \,. \qquad \ldots(24b)$$

Using condition (17) in (24a) and (24b) at *y = 0*, we obtain:

$$\lambda_1 \varphi_1^{\,2} \mu_1 b_1 \sqrt{-\beta_1} = \lambda_2 \varphi_2^{\,2} \mu_2 b_2 \sqrt{-\beta_2} \,. \qquad \ldots(25)$$

Solving (25) for b_1, we obtain:

$$b_1 = A_3 b_2 \qquad \ldots(26)$$

where

$$A_3 = \frac{\varphi_2^{\,2} \mu_2 \sqrt{\dfrac{k_1 \lambda_2}{k_2 \lambda_1}}}{\varphi_1^{\,2} \mu_1} \,. \qquad \ldots(27)$$

Equations (21a), (21b), (23), and (26) represent 4 equations in the 4 unknowns a_1, a_2, b_1, b_2. Solution to these equations takes the following form:

$$b_2 = \frac{A_4 A_5 \sec h A_1 - A_5 \sec h A_2 - A_7}{A_4 A_3 \tanh A_1 + \tanh A_2} \qquad \ldots(28a)$$

$$b_1 = \frac{A_3 A_4 A_5 \sec h A_1 - A_3 A_5 \sec h A_2 - A_3 A_7}{A_4 A_3 \tanh A_1 + \tanh A_2} \qquad \ldots(28b)$$

$$a_1 = (A_3 \tanh A_1)\left\{ \frac{A_4 A_5 \sec h A_1 - A_5 \sec h A_2 - A_7}{A_4 A_3 \tanh A_1 + \tanh A_2} \right\} - A_5 \sec h A_1 \qquad \ldots(28c)$$

$$a_2 = A_7 + A_4 \left[(A_3 \tanh A_1)\left\{ \frac{A_4 A_5 \sec h A_1 - A_5 \sec h A_2 - A_7}{A_4 A_3 \tanh A_1 + \tanh A_2} \right\} - A_5 \sec h A_1 \right] \qquad \ldots(28d)$$

where

W.S. Almalki Int. Journal of Engineering Research and Applications
www.ijera.com
ISSN: 2248-9622, Vol. 6, Issue 2, (Part - 5) February 2016, pp.10-21

$$A_4 = \frac{\varphi_1}{\varphi_2} \qquad \qquad \text{…(29a)}$$

$$A_5 = \lambda_1 Q_1 \qquad \qquad \text{…(29b)}$$

$$A_6 = \lambda_2 Q_2 \qquad \qquad \text{…(29c)}$$

$$A_7 = A_4 A_5 - A_6. \qquad \qquad \text{…(29d)}$$

Once values of the constants a_1, a_2, b_1, b_2, above, are obtained and substituted in (18a) and (18b), the velocity profile in each layer becomes completely determined. Using the values of the constants in (24a) and (24b) yields the shear stress across each layer.

III.1. Velocity and Shear Stress at the Interface

At $y = 0$, equations (2.18a) and (2.18b) yield, respectively, the following values of velocity at the interface:

$$u_1(0) = a_1 + \lambda_1 Q_1 \qquad \qquad \text{…(31)}$$

$$u_2(0) = a_2 + \lambda_2 Q_2. \qquad \qquad \text{…(32)}$$

Relationship between these velocities is given by equation (15). Either of equations (31) or (32) can be used to compute the velocity at the interface as follows. Letting u_i be the velocity at the interface then, we set:

$$u_i = \varphi_1 u_1(0) = \varphi_1(a_1 + \lambda_1 Q_1) = \varphi_1(a_1 + A_5) \qquad \qquad \text{…(33a)}$$

or

$$u_i = \varphi_2 u_2(0) = \varphi_2(a_2 + \lambda_2 Q_2) = \varphi_2(a_2 + A_6). \qquad \qquad \text{…(33b)}$$

Equations (33a) and (33b) show the dependence of the velocity at the interface on the Darcy numbers, Darcy velocities of the fluids, porosities, viscosities and viscosity factors of the saturating fluids, and the thickness of each layer. In addition, velocity distribution in each layer is dependent upon these same parameters. In particular, if $L_2 = 0$, or equivalently the upper layer is of zero thickness, equation (18a) renders the following velocity profile through a single porous layer (the lower layer):

$$u_1 = -\lambda_1 Q_1 \left[\frac{\cosh\sqrt{-\beta_1}\, y}{\mathrm{sec}h\sqrt{-\beta_1} L_1} - 1 \right]. \qquad \qquad \text{…(34)}$$

Shear force exerted by each layer is given by equation (16), namely $\lambda_i \varphi_i^2 \mu_i \dfrac{du_i}{dy}$, $i=1, 2$. At the interface, $y = 0$, the shear forces are equal. Expressions for $\dfrac{du_i}{dy}$ are given by equations 24 (a) and 24(b). At $y = 0$, layer1 exerts the following shear force (S.F.) on layer 2:

$$S.F. = \lambda_1 \varphi_1^2 \mu_1 b_1 \sqrt{-\beta_1}. \qquad \qquad \text{…(35)}$$

III.2. Relationships between the Darcy velocities in the layers

Assuming that the driving pressure gradient is the same constant in each of the layers, that is

$$\frac{dp_1}{dx} = \frac{dp_2}{dx} \qquad \qquad \text{…(36)}$$

then, using equation (7), we get:

$$\frac{\lambda_1 \mu_1 \varphi_1 Q_1}{k_1} = \frac{\lambda_2 \mu_2 \varphi_2 Q_2}{k_2}. \qquad \qquad \text{…(37)}$$

If $\mu_1 = \mu_2$ then (37) reduces to:

$$\frac{\lambda_1 \varphi_1 Q_1}{k_1} = \frac{\lambda_2 \varphi_2 Q_2}{k_2}. \qquad \qquad \text{…(38)}$$

If $\varphi_1 = \varphi_2$ and $\lambda_1 = \lambda_2$ then (38) reduces to

W.S. Almalki Int. Journal of Engineering Research and Applications
ISSN: 2248-9622, Vol. 6, Issue 2, (Part - 5) February 2016, pp.10-21

www.ijera.com

$$\frac{Q_2}{k_2} = \frac{Q_1}{k_1}.$$ …(39)

Equation (39) gives a relationship between the Darcy velocities in two layers of differing permeability.

III.3. Velocity and Shear Stress at the Interface: Results and Discussion

Determination of the velocity at the interface can be carried out according to the following steps:

Step 1: Given the porosity of each layer, determine the viscosity factors, λ_i, using equation (3).

As a first approximation, we follow [5] and use Einstein's formula to relate fluid viscosity and the effective viscosity:

$$\mu_i^* = [1 + \frac{5}{2}(1 - \varphi_i)]\mu_i. \quad …(40)$$

Table 1, below, is produced using equations (3) and (40) and shows the viscosity factor for selected high values of porosity. It shows that the quadratic increase in the viscosity factor with a decrease in porosity.

φ_i	0.65	0.7	0.8	0.9	0.95	0.98	0.99	1
λ_i	4.437869822	3.571	2.34375	1.543	1.246	1.09329446	1.0458	1

Table 1. Viscosity Factor λ_i Based on Einstein's Law for Viscosity of a Suspension

Step 2: Determine the Darcy number, Da_i, for each layer. This is accomplished as follows.

For a given porosity and average solid grain diameter, d_i, for each layer, compute the permeability in each layer using the following relationship between permeability and porosity is given by [17]:

$$k_i = \frac{\varphi_i^3 d_i^2}{150(1 - \varphi_i)^2}$$ … (41)

Then, for each layer thickness, L_i, compute $Da_i = \frac{k_i}{L_i^2}$. **Table 2** is produced using (41) for selected values of

porosity and grain diameter and demonstrates the dependence of permeability on these values. It shows that for a given porosity, the permeability decreases with decreasing grain diameter. For a given grain diameter, decrease in porosity results in decrease in permeability.

φ_i	d_i	k_i
0.98	10^{-3}	$1.568653333 \times 10^{-5}$
0.98	10^{-4}	$1.568653333 \times 10^{-7}$
0.65	10^{-3}	$1.494557823 \times 10^{-8}$
0.65	10^{-4}	$1.494557823 \times 10^{-10}$
0.6	10^{-3}	9×10^{-9}
0.6	10^{-4}	9×10^{-11}
0.5	10^{-3}	$3.333333333 \times 10^{-9}$
0.5	10^{-4}	$3.333333333 \times 10^{-11}$

Table 1 Permeability Values for Selected Porosity Values and Grain Diameter

Tables 3 and **4** illustrate the Darcy numbers that correspond to a given permeability and layer thickness, and demonstrate the quadratic decrease of Darcy number with increasing layer thickness. It is clear that Darcy number increases with increasing permeability for a given layer thickness.

k_i	Da_i when $L_i = 0.001$	Da_i when $L_i = 0.01$	Da_i when $L_i = 0.1$
$1.568653333 \times 10^{-5}$	15.68653333	0.1568653333	0.001568653333
$1.568653333 \times 10^{-7}$	0.1568653333	0.001568653333	0.00001568653333
$1.494557823 \times 10^{-8}$	0.01494557823	0.0001494557823	0.000001494557823
$1.494557823 \times 10^{-10}$	0.0001494557823	0.000001494557823	$1.494557823 \times 10^{-8}$

9×10^{-9}	0.009	9×10^{-5}	9×10^{-7}
9×10^{-11}	0.00009	9×10^{-7}	9×10^{-9}
$3.333333333 \times 10^{-9}$	0.003333333333	$3.333333333 \times 10^{-5}$	$3.333333333 \times 10^{-7}$
$3.333333333 \times 10^{-11}$	0.00003333333333	$3.333333333 \times 10^{-7}$	$3.333333333 \times 10^{-9}$
$1.185185185 \times 10^{-9}$	0.001185185185	0.00001185185185	$1.185185185 \times 10^{-7}$
$1.185185185 \times 10^{-11}$	0.00001185185185	$1.185185185 \times 10^{-7}$	$1.185185185 \times 10^{-9}$
$1.062778823 \times 10^{-9}$	0.001062778823	0.00001062778823	$1.062778823 \times 10^{-7}$
$1.062778823 \times 10^{-11}$	0.00001062778823	$1.062778823 \times 10^{-7}$	$1.062778823 \times 10^{-9}$
$3.673469388 \times 10^{-10}$	0.0003673469388	0.000003673469388	$3.673469388 \times 10^{-8}$
$3.673469388 \times 10^{-12}$	0.000003673469388	$3.673469388 \times 10^{-8}$	$3.673469388 \times 10^{-10}$
$1.851851852 \times 10^{-10}$	0.0001851851852	0.000001851851852	$1.851851852 \times 10^{-8}$
$1.851851852 \times 10^{-12}$	0.000001851851852	$1.851851852 \times 10^{-8}$	$1.851851852 \times 10^{-10}$
$8.230452675 \times 10^{-12}$	0.000008230452675	$8.230452675 \times 10^{-8}$	$8.230452675 \times 10^{-10}$
$8.230452675 \times 10^{-14}$	0.0000000823045676	$8.230452675 \times 10^{-10}$	$8.230452675 \times 10^{-12}$

Table 3 Darcy Number for Different Permeability and Layer Thickness

k_i	Da_i when $L_i = 0.5$	Da_i when $L_i = 1$
$1.568653333 \times 10^{-5}$	0.00006274613332	$1.568653333 \times 10^{-5}$
$1.568653333 \times 10^{-7}$	$6.274613332 \times 10^{-7}$	$1.568653333 \times 10^{-7}$
$1.494557823 \times 10^{-8}$	$5.978231292 \times 10^{-8}$	$1.494557823 \times 10^{-8}$
$1.494557823 \times 10^{-10}$	$5.978231292 \times 10^{-10}$	$1.494557823 \times 10^{-10}$
9×10^{-9}	3.6×10^{-8}	9×10^{-9}
9×10^{-11}	3.6×10^{-10}	9×10^{-11}
$3.333333333 \times 10^{-9}$	$1.333333333 \times 10^{-8}$	$3.333333333 \times 10^{-9}$
$3.333333333 \times 10^{-11}$	$1.333333333 \times 10^{-10}$	$3.333333333 \times 10^{-11}$
$1.185185185 \times 10^{-9}$	$4.740740740 \times 10^{-9}$	$1.185185185 \times 10^{-9}$
$1.185185185 \times 10^{-11}$	$4.740740740 \times 10^{-11}$	$1.185185185 \times 10^{-11}$
$1.062778823 \times 10^{-9}$	$4.251115292 \times 10^{-9}$	$1.062778823 \times 10^{-9}$
$1.062778823 \times 10^{-11}$	$4.251115292 \times 10^{-11}$	$1.062778823 \times 10^{-11}$
$3.673469388 \times 10^{-10}$	$1.469387755 \times 10^{-9}$	$3.673469388 \times 10^{-10}$
$3.673469388 \times 10^{-12}$	$1.469387755 \times 10^{-11}$	$3.673469388 \times 10^{-12}$
$1.851851852 \times 10^{-10}$	$7.407407408 \times 10^{-10}$	$1.851851852 \times 10^{-10}$
$1.851851852 \times 10^{-12}$	$7.407407408 \times 10^{-12}$	$1.851851852 \times 10^{-12}$
$8.230452675 \times 10^{-12}$	$3.292181070 \times 10^{-11}$	$8.230452675 \times 10^{-12}$
$8.230452675 \times 10^{-14}$	$3.292181070 \times 10^{-13}$	$8.230452675 \times 10^{-14}$

Table 4   Darcy Number for Different Permeability and Layer Thickness

Step 3: For a given constant driving pressure gradient, $\dfrac{dp_i}{dx}$, and given the fluid base viscosity, μ_i , compute

Q_i using equation (7).

The values of Q_i are illustrated in **Table 5** for the range of permeability considered and for different values of pressure gradient. For the sake of illustration, we consider the flowing fluid to be water at a temperature of $20^{\circ}C$ with a dynamic viscosity of $\mu = 1.002 \times 10^{-3} \, pa.s.$ (Pascal Second), density $\rho = 99829 \, kg/m^3$ and

kinematic viscosity of $\nu = \dfrac{\mu}{\rho} = 1.004 \times 10^{-6} m^2 / s.$ **Table 5** demonstrates the expected increase in flow

rate, Q_i, with increasing pressure gradient for a given permeability, and the increase in flow rate with increasing permeability for a given pressure gradient.

k_i	φ_i	λ_i	Q_i when $\dfrac{dp_i}{dx} = -10^2$	Q_i when $\dfrac{dp_i}{dx} = -10^{-1}$
$1.568653333 \times 10^{-5}$	0.98	1.093294460	1.461154137	0.1461154137
$1.568653333 \times 10^{-7}$	0.98	1.093294460	0.01461154137	0.001461154137
$1.494557823 \times 10^{-8}$	0.65	4.437869822	0.0005170792203	0.00005170792203
$1.494557823 \times 10^{-10}$	0.65	4.437869822	0.000005170792203	$5.170792203 \times 10^{-7}$
9×10^{-9}	0.6	5.555555555	0.0002694610778	0.00002694610778
9×10^{-11}	0.6	5.555555555	0.000002694610778	$2.694610778 \times 10^{-7}$
$3.333333333 \times 10^{-9}$	0.5	9	0.00007392622162	0.000007392622162
$3.333333333 \times 10^{-11}$	0.5	9	$7.392622162 \times 10^{-7}$	$7.392622162 \times 10^{-8}$
$1.185185185 \times 10^{-9}$	0.4	15.6250	0.00001892511274	0.000001892511274
$1.185185185 \times 10^{-11}$	0.4	15.6250	$1.892511274 \times 10^{-7}$	$1.892511274 \times 10^{-8}$
$1.062778823 \times 10^{-9}$	0.39	16.60092044	0.00001638243280	0.000001638243280
$1.062778823 \times 10^{-11}$	0.39	16.60092044	$1.638243280 \times 10^{-7}$	$1.638243280 \times 10^{-8}$
$3.673469388 \times 10^{-10}$	0.3	30.55555556	0.000003999422307	$3.999422307 \times 10^{-7}$
$3.673469388 \times 10^{-12}$	0.3	30.55555556	$3.999422307 \times 10^{-8}$	$3.999422307 \times 10^{-9}$
$1.851851852 \times 10^{-10}$	0.25	46	0.000001607091775	$1.607091775 \times 10^{-7}$
$1.851851852 \times 10^{-12}$	0.25	46	$1.607091775 \times 10^{-8}$	$1.607091775 \times 10^{-9}$
$8.230452675 \times 10^{-12}$	0.1	325	$2.527392193 \times 10^{-8}$	$2.527392193 \times 10^{-9}$
$8.230452675 \times 10^{-14}$	0.1	325	$2.527392193 \times 10^{-10}$	$2.527392193 \times 10^{-11}$

Table 5   Values of Q_i for Different Pressure Gradients

Step 4: Compute velocity at the interface using (33a) or (33b) using the data computed in Steps 1, 2, and 3.
In order to understand the effects of the physical parameters on the velocity at the interface, we consider the effects of layer thickness, pressure gradient, and the effects of permeability, porosity and Darcy number of each layer.

Effect of Layer Thickness
In order to illustrate the effect of layer thickness, we consider water in both layers with

$\mu_1 = \mu_2 = 1.002 \times 10^{-3}$. We also fix the following parameters:

$\varphi_1 = \varphi_2 = 0.98$; $d_1 = d_2 = 10^{-3}$; $\lambda_1 = \lambda 2_2 = 1.093294460$; $\dfrac{dp_1}{dx} = \dfrac{dp_2}{dx} = -10^2$;

$k_1 = k_2 = 1.568653333 \times 10^{-5}$; $Q_1 = Q_2 = 1.461154137$.

We then take $L_1 = 0.5$ and vary L_2 to take the values $L_2 = 0.001$; 0.01; 0.1; 0.5; 1, and calculate the

corresponding values of Da_2 . Results of these calculations are given in **Table 4**.

Upon using expressions (26)-(30), we produce the following Table of coefficients, and evaluate the velocity,

u_i , and shear force, S.F., at the interface using (33(a)) and (35), respectively.

Table 6 demonstrates the increase in the velocity at the interface as the lower layer thickness increases relative to the upper layer thickness. The increase continues until the two layers are of the same thickness, and further increase in the lower layer thickness does not affect the velocity at the interface.
The above increase in velocity at the interface is accompanied with a decrease of the absolute value of the shear force to the point where the two layers are of equal thickness. At this point, the shear force becomes negligibly

small and continues to be negligible for further increase in the lower layer thickness. The apparent vanishing of the shear force with increasing lower layer thickness could be attributed to the low permeability used in the current model, and is indicative of the need to consider higher values of permeability if the current model is used. For low permeability (low Darcy number), the model behaves like a Darcy model, characterized by the absence of shear force in the study of flow through two layers.

L_2	0.001	0.01	0.1	0.5	1
u_i	0.3358510411	1.425577450	1.565522289	1.565522289	1.565522289
S.F.	-0.3187863	-0.036279	-0.1322×10^{-10}	0	0

Table 6 Effect of Layer Thicknesses on Velocity and Shear Force at the Interface.

Effect of Pressure Gradient

In order to illustrate the effect of the pressure gradient on the velocity at the interface, we consider the following two cases:

Case 1: Pressure gradients are equal in the two layers.

Case 2: Pressure gradient in one layer is higher than the pressure gradient in the other layer.

In both cases, we fix all other parameters by taking:

$$L_1 = L_2 = 0.5$$
$$\mu_1 = \mu_2 = 1.002 \times 10^{-3}$$
$$\varphi_1 = \varphi_2 = 0.98$$
$$d_1 = d_2 = 10^{-3}$$
$$\lambda_1 = \lambda_2 = 1.093294460$$
$$k_1 = k_2 = 1.568653333 \times 10^{-5}$$
$$Q_1 = Q_2 = 1.461154137$$
$$\mu_1 = \mu_2 = 1.002 \times 10^{-3}$$
$$Da_1 = Da_2 = 6.274613332 \times 10^{-5}$$

In Case 1 we take $\dfrac{dp_1}{dx} = \dfrac{dp_2}{dx} = -10^2$, and in Case 2 we take $\dfrac{dp_1}{dx} = -10^2$ and $\dfrac{dp_2}{dx} = -10^{-1}$.

	$\dfrac{dp_1}{dx} = \dfrac{dp_2}{dx} = -10^2$	$\dfrac{dp_1}{dx} = -10^2$; $\dfrac{dp_2}{dx} = -10^{-1}$
u_i	1.565522289	0.8610372588

Table 7 Effect of Pressure Gradients on Velocity at the Interface.

Table 7 demonstrates a decrease in the velocity at the interface as the pressure in one layer is decreases. Clearly, the highest velocity occurs when the driving pressure gradients are equal in both layers. A decrease in the driving pressure gradient in one layer results in slower flow in that layer. This effect is transmitted across the interface (momentum transfer) and results in slowing down the flow in the other layer. Velocity continuity at the interface mandates that the flow is slower at the interface.

Effect of Darcy Number

In order to illustrate the effect of permeability, porosity and Darcy number, we consider the following cases:

Case 1: $Da_1 < Da_2$ and $\varphi_1 < \varphi_2$

Case 2: $Da_1 = Da_2$ and $\varphi_1 < \varphi_2$

In each case, we fix the following parameters:

$$L_1 = L_2 = 1$$
$$\frac{dp_1}{dx} = \frac{dp_2}{dx} = -10^2 .$$
$$\mu_1 = \mu_2 = 1.002 \times 10^{-3}$$
$$d_1 = d_2 = 10^{-3}$$

The combined effect of permeability, porosity, and layers thickness is illustrated by studying the effect of Darcy number. **Table 8** emphasizes the dependence of the velocity at the interface on Darcy number. Starting with equal values of Darcy number in each layer, velocity at the interface increases when the Darcy number is increased in one of the layers. This is due to the increase in flow velocity in the layer with higher permeability, thus increasing the momentum transfer across the interface. The end result is an increase in the velocity at the interface due to velocity continuity there.

	$\varphi_1 = 0.65 ; \varphi_2 = 0.98$ $\lambda_1 = 4.437869822$ $\lambda_2 = 1.093294460$ $Q_1 = 0.0005170792\ 203$ $Q_2 = 1.461154137$ $Da_1 = 1.494557823\ \times 10^{-8}$ $Da_2 = 1.568653333\ \times 10^{-5}$	$\varphi_1 = \varphi_2 = 0.65$ $\lambda_1 = \lambda_2 = 4.437869822$ $Q_1 = Q_2 = 0.0005170792\ 203$ $Da_1 = Da_2 = 1.494557823\ \times 10^{-8}$
u_i	0.03680295102	0.001491574674

Table 8 Effect of Darcy Number on Velocity at the Interface.

IV. CONCLUSION

In this work, we considered the flow of two viscous fluids through a two-layer porous medium. Appropriate matching conditions at the interface between the layers have been implemented to obtain the velocity distribution through the layers and to obtain an expression for the velocity at the interface. Equations 33(a,b) give the dimensionless velocity at the interface between the two layers and demonstrates the dependence of this velocity on the thicknesses of the layers; Darcy numbers; porosities; base viscosities of the fluids; Darcy velocities; and the viscosity factors. A four-step procedure is developed in this work to compute the necessary parameters and to determine the velocity at the interface. Results obtained support the formulation of the Brinkman model in the form given by equation (2) in the sense that this form better approximates Darcy's law when permeability is small. This work builds on, and provides details on the work reported in [18].

References

[1] K. Vafai and R. Thiyagaraja, Analysis of flow and heat transfer at the interface region of a porous medium, Int. J. Heat and Mass Transfer. 30(7), 1987, 1391-1405.

[2] G.S. Beavers and D.D. Joseph, Boundary conditions at a naturally permeable wall, J. Fluid Mechanics, 30(1), 1967, 197-207.

[3] B.C. Chandrasekhara, K. Rajani and N. Rudraiah, Effect of slip on porous-walled squeeze films in the presence of a magnetic field, Applied Scientific Research, 34, 1978, 393-411.

[4] M. Kaviany, Laminar flow through a porous channel bounded by isothermal parallel plates, Int. J. Heat and MassTransfer, 28, 1985, 851-858.

[5] N. Rudraiah, Flow past porous layers and their stability, Encyclopedia of Fluid Mechanics, Slurry Flow Technology, Gulf Publishing, Chapter 14, 1986, 567-647.

[6] H.C. Chan, W.C. Huang, J.M. Leu and C.J. Lai, Macroscopic modelling of turbulent flow over a porous medium, Int. J. Heat and Fluid Flow, 28(5), 2007, 1157-1166.

[7] E. Keramaris and P. Prinos, Flow characteristics in open channels with a permeable bed, J. Porous Media, 12(2), 2009, 155-165.

[8] P. Prinos, D. Sofialidis and E. Keramaris, Turbulent flow over and within a porous bed, J. Hydr. Engineering, 129(9), 2003, 720-733.

[9] H.C. Brinkman, A Calculation of the viscous force exerted by a flowing fluid on a dense swarm of particles, Applied Scientific Research, A1, 1947, 27-34.

[10] J.L. Auriault, On the domain of validity of Brinkman's equation, Transport in Porous Media, 79, 2009, 215–223.

[11] G. Neale, G. and W. Nader, Practical significance of Brinkman's extension of Darcy's law: coupled parallel Flows within a channel and a bounding porous medium, Canadian J. Chemical Engineering, 52, 1974, 475-478.

[12] M. Parvazinia, V. Nassehi, R. J. Wakeman, and M. H. R. Ghoreishy, Finite element modelling of flow through a porous medium between two parallel plates using the Brinkman equation, Transport in Porous Media, 63, 2006, 71–90.

[13] N. Rudraiah, Coupled parallel flows in a channel and a bounding porous medium of finite thickness, J. Fluids Engineering, ASME, 107, 1985, 322-329.

[14] F.M. Allan and M.H. Hamdan, Fluid mechanics of the interface region between two porous layers, J. Applied Mathematics and Computation, 128(1), 2002, 37-43.

[15] R.A.F ord and M.H. Hamdan, Coupled parallel flow through composite porous layers, J. Applied Mathematics and Computation, 97, 1998, 261-271.

[16] W.O. Williams, Constitutive equations for a flow of an incompressible viscous fluid through a porous medium, Quarterly of Applied Mathematics, Oct., 1978, 255-267.

[17] K. Vafai, Analysis of the channeling effect in variable porosity media, ASME J. Energy Resources and Technology, 108, 1986, 131–139.

[18] W.S. Almalki, M.H. Hamdan and M.T. Kamel, Analysis of Flow through Layered Porous Media, Proceedings of the 12th WSEAS International Conference on Mathematical Methods, Computational Techniques and Intelligent systems, ISBN: 978-960-474-188-5, 2010, 182-191.